Nucleic Acids Research, 1994, Vol. 22, No. 23 5139–5147

Mutational analysis of an essential binding site for the U3 snoRNA in the 5′ external transcribed spacer of yeast pre-rRNA

Monica Beltrame*, Yves Henry[1,+] and David Tollervey[1]
Dipartimento di Genetica e di Biologia dei Microrganismi, Universita' degli Studi di Milano, Via Celoria 26, 20133 Milan, Italy and [1]EMBL, Meyerhofstrasse 1, 69117 Heidelberg, Germany

Received July 28, 1994; Accepted August 30, 1994

ABSTRACT

The small nucleolar RNA U3 is essential for viability in yeast. We have previously shown that U3 can be cross-linked *in vivo* to the pre-rRNA in the 5′ external transcribed spacer (ETS), at +470. This ETS region contains 10 nucleotides of perfect complementarity to U3. In a genetic background where the mutated rDNA is the only transcribed rDNA repeat, the deletion of the 10 nt complementary to U3 is lethal. Cells lacking the U3 complementary sequence in pre-rRNA fail to accumulate 18S rRNA: pre-rRNA processing is inhibited at sites A0 in the 5′ ETS, A1 at the 5′ end of 18S rRNA and A2 in ITS1. We show here that effects on processing at site A0 are specific for U3 and its associated proteins and are not seen on depletion of other snoRNP components. The deletion of the sequence complementary to U3 in the ETS therefore mimics all the known effects of the depletion of U3 in trans. This indicates that we have identified an essential U3 binding site on pre-rRNA, required in cis for the maturation of 18S rRNA.

INTRODUCTION

In eukaryotic cells, transcription, processing and assembly of rRNA into ribosomal subunits are overlapping processes which occur mainly in a specialized nuclear compartment, the nucleolus. The ribosomal RNAs 18S, 5.8S and 25/28S are transcribed by RNA polymerase I as a single precursor molecule, in which rRNA coding regions are embedded in non-coding regions called spacers (see Fig. 1). The mature rRNA species are subsequently generated through a series of processing steps that eliminate the 5′ and 3′ external transcribed spacers (5′ ETS and 3′ ETS, respectively) and internal transcribed spacers 1 and 2 (ITS1 and 2, respectively). In principle, the essential processing machinery could consist of endonucleases which recognize and cleave the ends of the mature rRNA sequences. It is, however, clear that, at least in yeast, the pathway of pre-rRNA processing is substantially more complex than this, and obligatorily requires both the recognition and cleavage of sequences in the spacer regions.

Large deletions in the 5′ ETS in yeast prevent the synthesis of 18S rRNA but not 25S rRNA (1). In contrast, large deletions in ITS2 prevent the synthesis of 25S rRNA but not 18S rRNA (2). In addition, the precise removal of ITS2 from the rDNA does not allow the accumulation of the 5.8S/25S RNA, perhaps because the presence of the spacer is required for the assembly of the large ribosomal subunits (3). Deletions in ITS1 can affect the accumulation of either 18S or 25S and 5.8S rRNAs (1, 4, 5). The spacer regions, although apparently much less conserved than the mature rRNA sequences during evolution, seem therefore to contain essential cis-acting elements for the maturation of ribosomal subunits.

The small nucleolar RNAs (snoRNAs) are a class of nuclear RNAs which differ from the nucleoplasmic snRNAs in their nucleolar localization, association with nucleolar proteins, association with pre-rRNA species (for a review see 6) and biosynthetic pathway (7, 8). The snoRNAs and associated proteins act as trans-acting factors in the processing of pre-rRNA and, potentially, in other steps of ribosome synthesis. Fifteen snoRNAs have been characterized to date in yeast, but only five RNA species (U3, U14, snR10, snR30 and MRP RNA) have been shown to play a direct role in pre-rRNA processing (9–13). The depletion of any of several snoRNP components (the snoRNAs U3, U14, snR10 and snR30, or the proteins Nop1p, Sof1p and Gar1p) results in a similar defect in pre-rRNA processing. Normal intermediates in the pathway leading to 18S rRNA are missing and 18S rRNA is underaccumulated, whereas 25S and 5.8S are normally synthesized (9–12, 14–16). The similarities in the phenotypes of the mutants suggest that these snoRNPs are associated in a multi-snoRNP processing complex which cleaves sites A1 and A2 (see Fig. 1) in a coordinated manner.

U3 has also been implicated in pre-rRNA processing in vertebrates. In *Xenopus* oocytes, removal of the 5′ third of U3 snoRNA has been reported to interfere with cleavage at the boundary of ITS1 and 5.8S rRNA (17). *In vitro* cleavage of the

*To whom correspondence should be addressed

+Present address: Institut de Biologie Cellulaire et de Génétique du CNRS, LBME, 118 route de Narbonne, 31062 Toulouse cedex, France

5′ ETS in mouse and *Xenopus* cell extracts also requires U3; processing is inhibited by depletion of the U3 snoRNP by immunoprecipitation or by oligonucleotide-directed cleavage of the U3 snoRNA (18, 19). This processing reaction is associated with the assembly of a large complex in mammalian (20) and *Xenopus* cell extracts (19). These putative processing complexes can be visualized as terminal balls on nascent RNA pol I transcripts (the so-called Christmas trees) by electron microscopy of chromatin spreads (21). The terminal knobs have been observed in a multitude of other species, including yeast (22), and are thought to be conserved across eukaryotic evolution (references in 21), despite the fact that the efficiency of ETS processing varies between species. The cleavage reaction in the 5′ ETS might be irrelevant for the maturation of rRNA, whereas the important conserved feature could be the formation of such complexes in the ETS to promote subsequent processing events.

In vivo psoralen cross-linking studies indicate that in rat (23) and human cells (24), U3 is associated with a region of the 5′ ETS including or adjacent to the U3-dependent primary processing site. By *in vivo* psoralen cross-linking, we have identified two sites in the yeast 5′ ETS, at +470 and +655, which contact the U3 snoRNA (25) (see Fig. 2). +655 is predicted to lie in the loop of an extended stem-loop structure (26), with the A0 and A1 cleavage sites at the base of this stem. The 5′ ETS region around +470 shows two interesting features: it contains 10 nt of perfect complementarity to yeast U3 snoRNA and it shows some homology to ETS sequences in other organisms (such as human, mouse, rat and *Xenopus*), including the U3-dependent early processing site reported in vertebrates. The cross-links in yeast U3 snoRNA are situated in the evolutionarily conserved box A sequence and at the border of the sequence which is complementary to the ETS and largely single-stranded (27). We showed that a deletion of 23 nt (Δ23, see Fig. 2) around +470, which eliminates the complementarity to U3 and most of the region of potential homology to the vertebrate 5′ ETS, causes a dramatic drop in the level of 18S rRNA, without affecting 25S rRNA synthesis. We therefore decided to better characterize this ETS region in yeast by a finer mutational analysis. Here we show that the deletion of the 10 nucleotides complementary to U3 in the yeast ETS is sufficient to block the synthesis of 18S rRNA, mimicking in cis all the known effects of U3 depletion in trans.

MATERIALS AND METHODS

Yeast strains

Yeast strain NOY504 (*MATα*, *rrn4::LEU2*, *ade2-101*, *ura3-1*, *trp1-1*, *leu2-3,112*, *can1-100*), generously provided by Dr M. Nomura, was used for all experiments involving *GAL7*-rDNA hybrid plasmids; this strain, carrying a disrupted *rrn4* (*rpa12*) gene, shows a ts phenotype due to inactivation of RNA polymerase I (28). Strain BWG1-7A (*MATa*, *ura3-52*, *leu2-3,112*, *ade1-100*, *his4-519*), generously provided by Dr L. Guarente, was used for chromosomal integration of ETS mutations.

Construction of ETS mutations

Mutagenesis was carried out by PCR essentially as described by Landt *et al.* (29). A tagged rDNA plasmid (pBSrDNA2× tagURA3-6, see 25) was used as template DNA. Each mutation was created by using two external oligonucleotides (corresponding to the ETS sequence +102/+120 from the transcription start site and to the 18S template DNA strand +56/+34) and a single mutagenic oligonucleotide. A *Bgl*II−*Hin*dIII digestion fragment containing the ETS mutations was cloned into a suitable tagged rDNA vector by substitution of the corresponding wt fragment and completely sequenced to discard random mutations introduced by Taq polymerase. A *Not*I−*Bam*HI fragment from this construct was cloned into plasmid pBSrDNA2×tagURA3-6 by substitution of the corresponding wt fragment. This plasmid was used as described for integration of the mutated rDNA into the chromosomal locus (25).

Alternatively, a *Bgl*II−*Bgl*II rDNA fragment from this plasmid was used to replace the corresponding fragment of pNOY102 (30), a *GAL7*-rDNA hybrid plasmid generously provided by Dr M. Nomura. This replacement introduces at the same time the ETS mutation and both 18S and 25S tags in the *GAL7*-rDNA hybrid plasmid. In the latter case, 10 μg of plasmid DNA were used to transform strain NOY504 by the Li-acetate method (31). The *GAL7*-rDNA hybrid plasmids carrying 18S and 25S tags were named according to the ETS mutation that was introduced: pΔ23 carries the Δ23 deletion in the ETS, whereas pwt has no mutation. The sequences of the mutagenic oligos are as follows:

Δ1, 5′-GATTAGAGGAAACCTATGGTATGGTGACGG-3′;
Δ2, 5′-AGAGGAAACTCAAAGAGTGTGGTGACGGAGTGCGC-3′;
Δ3, 5′-CAAAGAGTGCTATGGTAGAGTGCGCTGGTCAAG-3′;
Δ4, 5′-GGTATGGTGACGTGGTCAAGAGTGTAAAAGC-3′.

Northern hybridization

Yeast cells transformed with wild-type or mutated plasmids were grown in selective galactose liquid medium at 25°C until OD_{600} < 0.1, then shifted to 37°C for 6 h. Total RNA was extracted, run on 1.2% agarose-formaldehyde gels and transferred to Hybond membranes as described by Tollervey (9). RNA extracted from the same OD_{600} units of cells was loaded for each sample.

Northerns were hybridized with labelled oligonucleotides complementary to the tags or with oligonucleotides specific for pre-rRNA species (Fig. 1). The hybridization probe oligos are as follows: oligo b (5′-CGAGGATCCAGGCTTT-3′), complementary to 18S tag (Fig. 4); oligo g (5′-ACTCGAGAGC-TTCAGTAC-3′), complementary to 25S tag (Fig. 4); oligo c (5′-CGGTTTTAATTGTCCTA-3′), complementary to the 5′ region of ITS1 (Fig. 5A and D); oligo d (5′-ATGAAAACTCC-ACAGTG-3′), complementary to the 3′ region of ITS1 (Fig. 5B); oligo f (5′-GGCCAGCAATTTCAAGTTA-3′), complementary to ITS2 (Fig. 5C).

Primer extension

Cells were grown and RNA was extracted as for Northerns. Total RNA equivalent to 0.4−0.8 OD_{600} units of cells was used in each experiment.

Primer extensions were performed as described in Beltrame and Tollervey (25). The oligonucleotides used for the experiments shown in the figures were: oligonucleotides b and g complementary to the 18S and 25S tags, respectively (Fig. 6A and C; see Northern hybridization for sequences); oligo a (5′-CCAAATAA-CTATCTTAAAAG-3′), complementary to the 18S/ETS boundary (Fig. 6B); oligo e (5′-CCAGTTACGAAAATT-CTTG-3′), complementary to the 3′ region of ITS1 (Fig. 6D). For Fig. 7 an oligonucleotide complementary to nt +56/+34 of 18S rRNA was used (5′-CATGGCTTAATCTTTGAGAC-3′).

Although generally not shown in the figures, the same oligonucleotides were also kinased with unlabelled ATP and used

to generate dideoxy sequence ladders from plasmid DNA templates, which were run alongside the primer extension samples.

Pulse-chase labelling of RNA

Pre-rRNA was labelled with [^{3}H-methyl]methionine as described by Henry *et al.* (5) following 9 hours of incubation at 37°C.

RESULTS

Experimental design

To define the relevant elements of the ETS region around the U3 cross-linking site at +470, a set of four small deletions (8–10 nt) spanning the whole region of potential conservation was created by *in vitro* mutagenesis and the effects of these mutations were analyzed in detail *in vivo*. The deletions were designated Δ1 to Δ4 (see Fig. 2); Δ1 eliminates just the 10 nt of perfect complementarity to U3 including the *in vivo* cross-linking site at +470, while Δ2 covers 8 nt which are complementary to the 5′ end of snR30. This snoRNA was shown to be associated with the 35S pre-rRNA by *in vivo* psoralen cross-linking (12); the cross-linking sites have not yet been mapped at the nucleotide level, but the complementarity between the 5′ region of snR30 and the ETS region immediately adjacent to the U3 cross-linking site suggested a potential snR30 binding site.

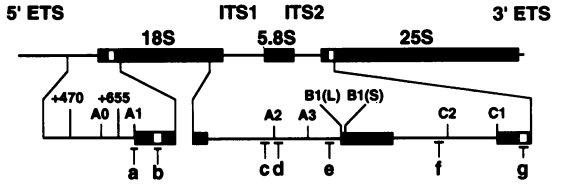

Figure 1. Structure of the 35S pre-rRNA. The locations of the oligonucleotides used for the analysis of the mutations in the pre-rRNA are indicated. Thick lines indicate the mature rRNA domains; open boxes within these indicate the sites of insertion of the tags. The positions of the pre-rRNA processing sites and of the U3 cross-linking sites are indicated.

The large number of rDNA repeat units in the yeast genome (150–200 copies) hampers a direct analysis of the effects of mutations in the pre-rRNA on processing. Two methods have been developed to overcome this problem. The first uses small oligonucleotide tags inserted in the rRNA coding regions to follow the fate of a single mutated rDNA unit either expressed from a plasmid (1, 32) or integrated into the rDNA chromosomal locus (25). This method allows the analysis of pre-rRNA transcribed within the nucleolus by the physiological RNA polymerase I (pol I). The analysis of the mutations is, however, limited to what can be seen from the tags which identify the products of the mutated rDNA unit. A kinetic analysis of the processing of the mutated pre-rRNA by pulse-chase would for example be impossible due to the high wild-type background. A second system is based on the expression of an rDNA repeat under the control of an inducible RNA polymerase II (pol II) promoter (30) in a strain carrying a ts mutation in pol I (28). The lethality of the pol I mutated strain at nonpermissive temperature can be suppressed by the galactose-induced pol II driven transcription of a wild-type pre-rRNA from a replicating plasmid. This system has been adapted to allow the analysis of the effects of mutations in the plasmid-borne rDNA unit on cell viability and pre-rRNA processing (5).

In this study, we made use of both systems to analyze the effects of ETS mutations on pre-rRNA processing. The deletions were created *in vitro* in an rDNA unit carrying short oligonucleotide tags in 18S and 25S coding sequences and a selectable marker in the non-transcribed spacer (see 25) and inserted in the

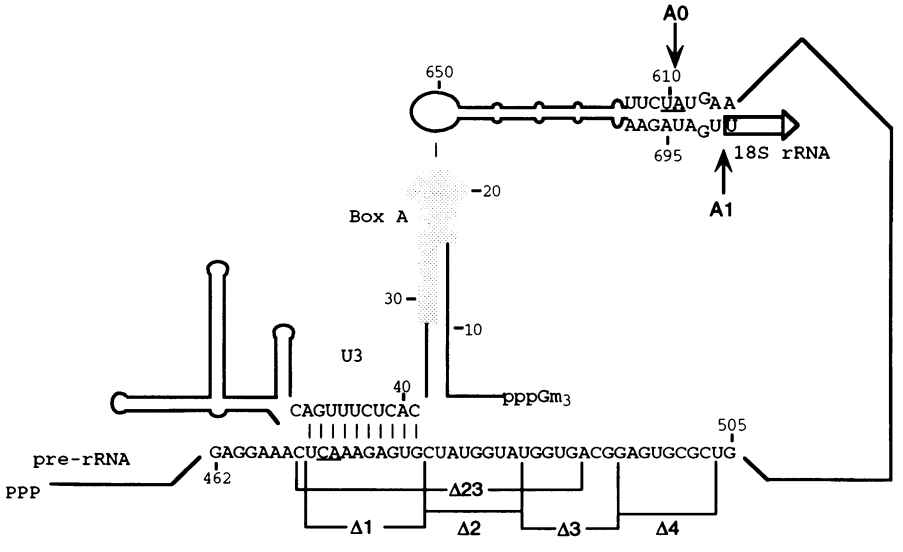

Figure 2. Mutations in the ETS region around +470. The ETS sequences deleted in the Δ23, Δ1, Δ2, Δ3, and Δ4 mutants are indicated below the sketch of the pre-rRNA. The complementarity between the U3 snoRNA and the ETS is marked by vertical bars. The evolutionarily conserved box A of U3 is indicated by a shaded region; the sketch of U3 secondary structure is not to scale. The 5′ end of the 18S rRNA sequence is boxed. Underlined nucleotides indicate strong primer extension stops in the ETS between nt +471/472 and +609/610; the latter corresponds to site A0, which is marked by an arrow. The A1 processing site is also indicated.

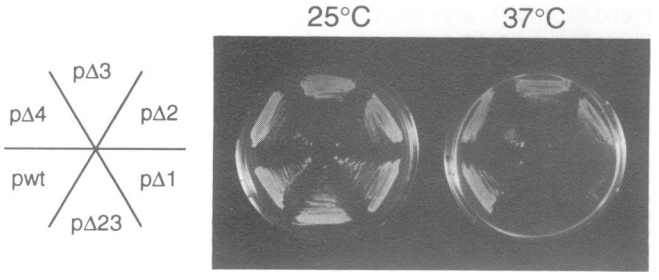

Figure 3. Effect of the ETS mutations on growth. Yeast pol I ts strains carrying either wt (pwt) or mutated (pΔ23, pΔ1, pΔ2, pΔ3 and pΔ4) *GAL7*-rDNA hybrid plasmids were streaked on galactose plates and incubated at permissive or nonpermissive temperature for the pol I mutation (25°C and 37°C, respectively). The positions of the strains are indicated on the left.

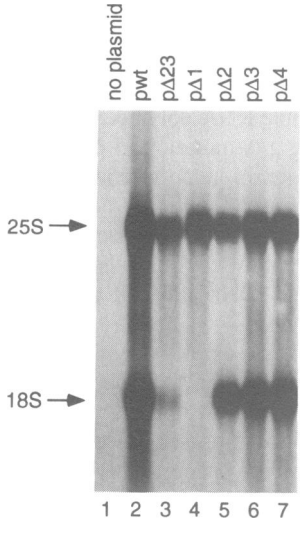

Figure 4. Effect of the ETS mutations on the steady-state levels of 18S and 25S rRNAs. The Northern filter was hybridized with oligonucleotide probes complementary to the tags in the mature 18S and 25S rRNAs (oligos b and g in Fig. 1). Lanes are: 1, RNA from an untransformed strain; 2, RNA from cells carrying pwt; 3, RNA from cells carrying pΔ23; 4, RNA from cells carrying pΔ1; 5, RNA from cells carrying pΔ2; 6, RNA from cells carrying pΔ3; 7, RNA from cells carrying pΔ4. All strains carry the pol I ts mutation. Total RNA was extracted from cells grown in galactose medium, 6h after shift to 37°C.

chromosomal rDNA repeat. In addition, the mutated portion of the rDNA containing the tags was inserted into an rDNA unit under the control of a *GAL7* promoter on a replicating plasmid and transformed into a pol I ts mutant strain. The plasmid expressing the wild-type pre-rRNA is designated pwt; plasmids expressing the pre-rRNA with the Δ1, Δ2, Δ3, Δ4 and Δ23 mutations are designated pΔ1, pΔ2 etc.

Deletions of the sequence complementary to U3 block 18S synthesis

The growth phenotype of the pol I ts strains, transformed with either wt or mutated *GAL7* plasmids, was directly scored on galactose plates incubated at permissive and nonpermissive temperature, 25°C and 37°C respectively. As shown in Fig. 3, all transformants are viable at 25°C. Plasmids containing the wt ETS or the Δ2, Δ3 and Δ4 mutations support growth at 37°C,

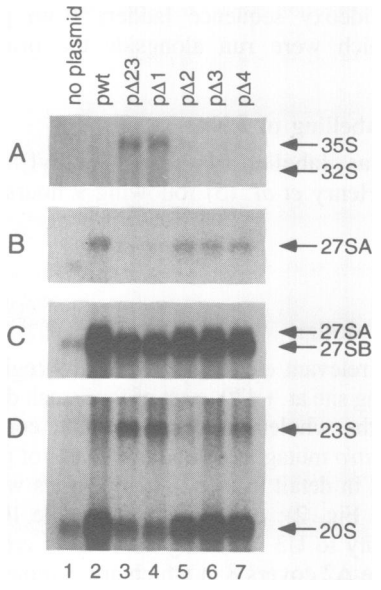

Figure 5. Effect of the ETS mutations on the steady-state levels of pre-rRNAs. Northern filters were hybridized with oligonucleotide probes specific for the pre-rRNAs. Only relevant parts of each Northern are shown and the positions of the major pre-rRNAs are indicated. Lanes are: 1, RNA from an untransformed strain; 2, RNA from cells carrying pwt; 3, RNA from cells carrying pΔ23; 4, RNA from cells carrying pΔ1; 5, RNA from cells carrying pΔ2; 6, RNA from cells carrying pΔ3; 7, RNA from cells carrying pΔ4. (**A**) and (**D**): hybridization with an oligo complementary to the 5′ region of ITS1 (oligo c in Fig. 1); different exposures are used in the two panels. (**B**): hybridization with an oligo complementary to the 3′ region of ITS1 (oligo d in Fig. 1). (**C**): hybridization with an oligo complementary to ITS2 (oligo f in Fig. 1). All strains carry the pol I ts mutation. Total RNA was extracted from cells grown in galactose medium, 6h after shift to 37°C.

in the absence of chromosomal rRNA transcription. In contrast, pΔ23 and pΔ1 cannot sustain growth at 37°C, indicating that the region of the 5′ ETS complementary to U3 is required for cell viability.

The tags inserted in 18S and 25S coding sequences were used to analyze the effect of the mutations on the steady state levels of mature rRNAs, 6 hours after shift to 37°C. As previously shown with a chromosomally integrated form of this mutation (25), the Δ23 deletion causes a dramatic drop in the level of 18S rRNA, without affecting the level of 25S rRNA (Fig. 4, lane 3). Surprisingly, the Δ1 deletion has an even more drastic effect on the level of 18S rRNA, which is almost undetectable by Northern analysis (Fig. 4, lane 4). The Δ2, Δ3 and Δ4 deletions have no effect on the steady state levels of either 18S or 25S rRNAs (Fig. 4, lanes 5 to 7). The same results were obtained when the mutated rDNAs (under the natural pol I promoter) were introduced in the chromosomal locus by gene replacement (data not shown).

We can therefore conclude that the inability to sustain growth shown by plasmids carrying deletions which eliminate the ETS sequence complementary to U3 (Δ23 and Δ1) is due to a block in 18S rRNA synthesis.

Deletions of the U3 complementary region in the ETS impair cleavage at sites A1 and A2

In order to better define the block in 18S rRNA synthesis caused by the Δ23 and Δ1 deletions and to be able to detect more subtle

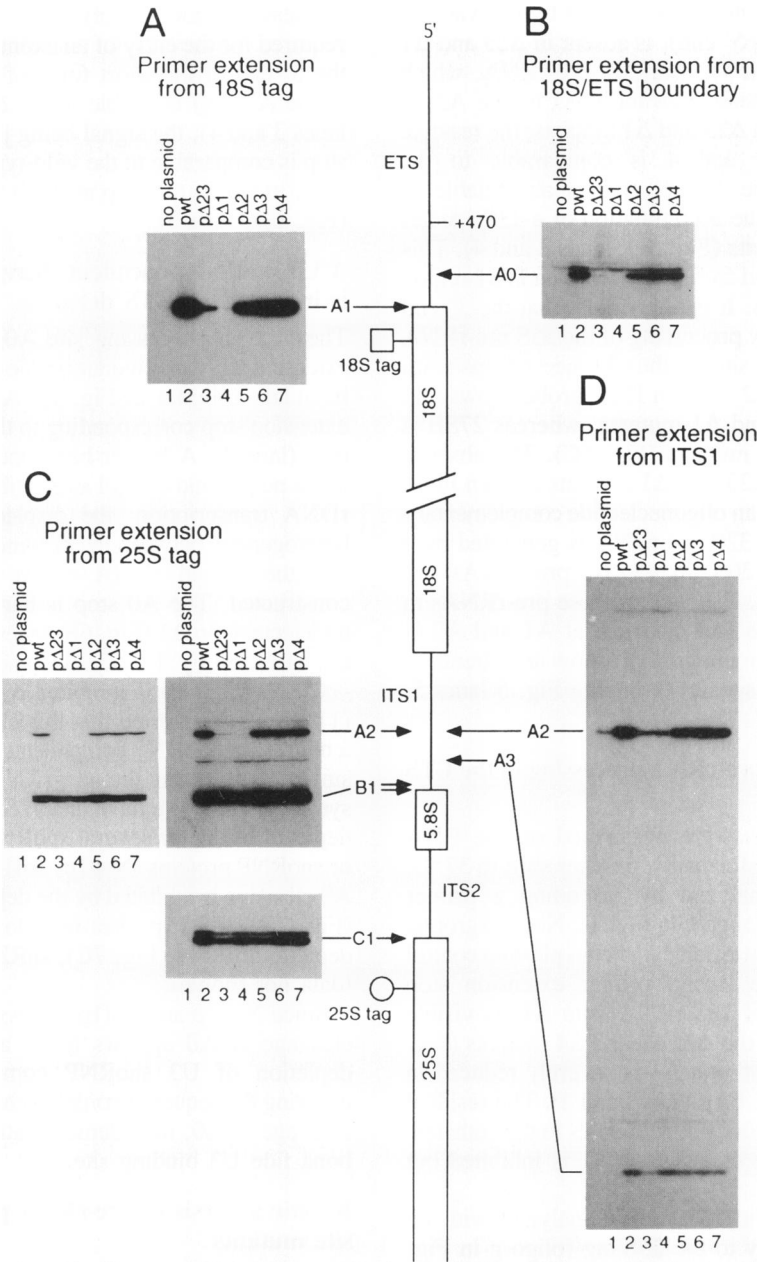

Figure 6. Effect of ETS mutations on pre-rRNA cleavage sites analyzed by primer extension. Primer extension reactions were run alongside a dideoxynucleotide sequence; the positions of cleavage sites derived from the sequences are indicated. The central drawing sketches part of the pre-rRNA primary transcript, from the ETS 5′ end to 25S rRNA. Spacer regions are drawn as simple lines, rRNA mature regions are drawn as blocks. The position of 18S and 25S tags are indicated by a square and a circle, respectively. The major processing sites are indicated by arrows; the ETS +470 region is also marked. In all panels lanes 1−7 are primer extensions with: 1, RNA from an untransformed strain; 2, RNA from cells carrying pwt; 3, RNA from cells carrying pΔ23; 4, RNA from cells carrying pΔ1; 5, RNA from cells carrying pΔ2; 6, RNA from cells carrying pΔ3; 7, RNA from cells carrying pΔ4. (**A**): primer extension from 18S tag. The A1 site is marked with an arrow pointing to the pre-rRNA scheme. The primer is oligo b in Fig. 1. (**B**): primer extension from 18S/ETS boundary. The A0 site is marked with an arrow pointing to the pre-rRNA scheme. The primer is oligo a in Fig. 1. (**C**): primer extension from 25S tag. The A2, B1, and C1 sites are marked with arrows pointing to the pre-rRNA scheme. Different exposures of the same gel are used to show primer extension stops of different intensities. The primer is oligo g in Fig. 1. (**D**): primer extension from ITS1. The A2 and A3 sites are marked with arrows pointing to the pre-rRNA scheme. The primer is oligo e in Fig. 1. All strains carry the pol I ts mutation. Total RNA was extracted from cells grown in galactose medium, 6h after shift to 37°C.

effects which might be caused by the other mutations, we performed a detailed analysis of pre-rRNA processing by Northern hybridization and primer extension.

RNA was extracted from the pol I ts strains transformed with the plasmids expressing the wild-type and mutant pre-rRNAs, 6 hours after shift to 37°C. Steady-state levels of the processing intermediates were assessed by Northern hybridization with probes specific for the pre-rRNAs (Fig. 5). The Δ23 and Δ1 deletions cause an accumulation of the 35S primary transcript (Fig. 5A, lanes 3 and 4), showing that the processing is slowed.

The 32S pre-rRNA, which is normally formed by cleavage of 35S pre-rRNA at site A1 (18S 5′ end), is absent in Δ23 and Δ1 mutants (Fig. 5A, lanes 3 and 4). The 20S pre-rRNA, which shares the 18S 5′ end and extends into the ITS1 to site A2, is reduced to background level in Δ23 and Δ1 mutants; the residual signal in Fig. 5D lanes 3 and 4 is comparable to the untransformed control in lane 1, and is thus attributable to chromosomal transcription. The accumulation of a 23S species is visible in Δ23 and Δ1 mutants (Fig. 5D, lanes 3 and 4). This pre-rRNA was shown to extend from the ETS to an ITS1 region between sites A2 and B1 (12). It is very likely that the 3′ end of the 23S species is formed by processing of the 35S pre-rRNA at the recently identified A3 site in the absence of upstream cleavage at sites A0, A1 or A2 (5). An ITS2 probe shows that 27SA is not present in Δ23 and Δ1 mutants, whereas 27SB is present at normal level in all mutants (Fig. 5C). The absence of the 27SA intermediate in Δ23 and Δ1 mutants is even more clearly shown in Fig. 5B, with an oligonucleotide complementary to the 3′ region of ITS1. The 32S pre-rRNA is generated by a cleavage at site A1, while 20S and 27SA pre-rRNAs are generated by a cleavage at A2. The lack of these pre-rRNAs in Δ23 and Δ1 mutants indicates that cleavage at A1 and A2 is impaired. The Δ2, Δ3 and Δ4 mutants don't show any alteration in the level of any pre-rRNA species (compare Fig. 5 lanes 5, 6, 7 to wt in lane 2).

Primer extension analysis of pre-rRNA processing in the ETS mutants

A series of primer extensions were performed on the RNA extracted from the pol I ts transformants, 6h after shift to 37°C. Cleavage at A1 site was analyzed by extending a primer complementary to the 18S tag (oligo b in Fig. 1). No background from non-tagged 18S rRNA is detectable in the no plasmid control (Fig. 6A, lane 1). A single strong primer extension stop corresponding to the 5′ end of 18S rRNA (site A1) is visible in the wild-type sample and in the Δ2, Δ3 and Δ4 mutants (Fig. 6A, lanes 2 and 5 to 7). The stop at A1 is severely reduced in Δ23 and even more in Δ1 (Fig. 6A, lanes 3 and 4). The residual primer extension signal corresponds in both cases to the authentic 5′ end of 18S rRNA, i.e. the cleavage at A1 is inhibited but accurate.

Processing sites in ITS1 and ITS2 were analyzed with an oligonucleotide complementary to the 25S tag (oligo g in Fig. 1); results are shown in Fig. 6C. Strong stops in the wild-type sample correspond to the processing sites C1 (5′ end of 25S rRNA), B1(L) and B1(S) (5′ ends of the long and short forms of 5.8S rRNA, respectively), and A2 (Fig. 6C, lane 2). Cleavage at site C2 is not detected by primer extension from oligonucleotides which hybridize 3′ to C1. The stops at C1, B1(L) and B1(S) are not altered in any mutant. The stop at A2 is greatly reduced by the Δ23 deletion and it is barely detectable in the Δ1 mutant (Fig. 6C, lanes 3 and 4); the signal is comparable to wild type in the Δ2, Δ3 and Δ4 mutants (Fig. 6C, lanes 5 to 7).

A more detailed analysis of the processing in the ITS1 region around the A2 site was performed by primer extension from the 3′ end of ITS1 (oligo e in Fig. 1); results are shown in Fig. 6D. In this case, there is some background due to residual chromosomal transcription (see no plasmid control, Fig. 6D lane 1). The primer extension stops corresponding to sites A2 and A3 are seen in the wild type. The stop at site A3 is altered in snR30 depleted cells and in *rat1/xrn1* mutants (5). The A3 site is cleaved endonucleolytically by RNase MRP (13) and is required for the entry of an exonuclease activity which generates the 5′ end of the short form of 5.8S rRNA (5). A clear drop in the A2 stop is visible in the Δ23 and Δ1 mutants (Fig. 6D, lanes 3 and 4), the signal being just above background. The A3 stop is comparable to the wild-type control in all mutants except Δ23, in which the stop at A3 is somewhat reduced in intensity (Fig. 6D, lane 3).

A U3 snoRNP dependent cleavage in the 5′ ETS, at site A0, is inhibited by ETS deletions

The 5′ ETS processing site A0 was also analyzed by primer extension with an oligonucleotide complementary to the 18S/ETS boundary (oligo a in Fig. 1). As shown in Fig. 6B, a primer extension stop corresponding to the A0 site is present in the wild type (lane 2). A fainter band one nt 5′ to A0 is detectable also in the no plasmid control and attributable to residual chromosomal rDNA transcription; the displacement is due to a sequence heterogeneity between the chromosomal rDNA in the host strain and the cloned rDNA repeat in which the mutations are constructed. The A0 stop is barely visible in Δ23 and almost undetectable in Δ1 (Fig. 6B, lanes 3 and 4), whereas its intensity is unaffected by the Δ2, Δ3, and Δ4 mutations (lanes 5 to 7).

Cleavage at A0 is inhibited by depletion of the U3 snoRNA (11). It was suggested that this cleavage might be dependent on a number of snoRNP components whose depletion causes overall similar results on the pre-rRNA processing leading to 18S synthesis (11). We have analyzed processing at site A0 in cells depleted of one of several snoRNAs (U3, U14, snR10, snR30) or snoRNP proteins (Nop1p, Sof1p, Gar1p) by primer extension. A0 cleavage is inhibited by the depletion of U3 (Fig. 7A), Nop1p (Fig. 7D) or Sof1p (data not shown), but is not affected by the depletion of U14 (Fig. 7C), snR30 (Fig. 7B), snR10, or Gar1p (data not shown).

Since Nop1p and Sof1p are associated with U3, inhibition of cleavage at A0 appears to be a specific consequence of the depletion of U3 snoRNP components. Our ETS deletions covering the sequence complementary to U3, Δ23 and Δ1, inhibit cleavage at A0, thus demonstrating that we are dealing with a bona fide U3 binding site.

Kinetic analysis of pre-rRNA processing in the U3 binding site mutants

The Δ23 and Δ1 mutants were further examined by labelling with [^{3}H-methyl]methionine. The pulse-chase labelling was performed using the pol I ts strains transformed with pwt, pΔ23 and pΔ1, after 9h of incubation at 37°C. As a control for residual chromosomal rDNA transcription, labelling was also performed using a strain transformed with a plasmid lacking the rDNA insert. The accumulation of 35S is evident in both mutants, a faint 35S band being visible even at late chase time points (Fig. 8, lanes 9−11 and 13−15). 25S rRNA is synthesized with normal kinetics and the 27SB pre-rRNA, but not 27SA pre-rRNA, is detected. The synthesis of 18S rRNA is strongly inhibited in both mutants, but particularly in Δ1. The 20S pre-rRNA, which is seen in the earliest time point in the wild-type samples (Fig. 8, lane 5) is undetectable in either mutant. The aberrant 23S is detectable at a low level in both mutants only at later chase time points. An unidentified band, just below 23S, is present even in the no rDNA control; this does not correspond to any pre-rRNA species detected by Northern hybridization and

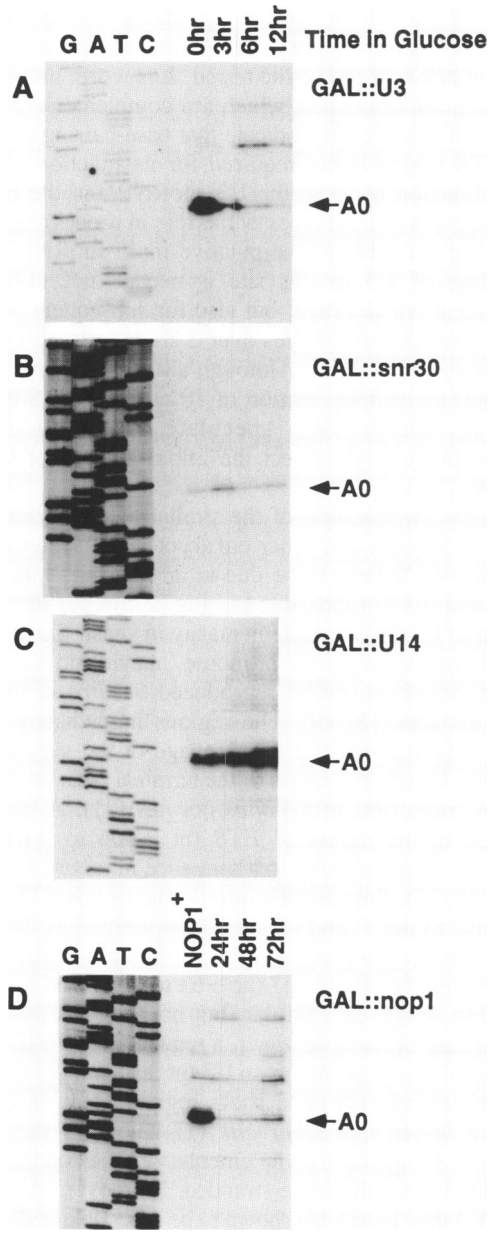

Figure 7. Primer extension through the A0 site in strains depleted of snoRNP components. Primer extensions were performed with an oligonucleotide complementary to 18S rRNA from +53 to +34, and the stop at A0 therefore represents ETS processing prior to cleavage at A1. (**A**): RNA extracted from a *GAL::U3* strain following growth on galactose medium and shift to glucose medium for the time indicated above each lane (0, 3, 6, 12 hours). (**B**): RNA extracted from a *GAL::snR30* strain following growth on galactose medium and shift to glucose medium for the time indicated above each lane (0, 3, 6, 12 hours). (**C**): RNA extracted from a *GAL::U14* strain following growth on galactose medium and shift to glucose medium for the time indicated above each lane (0, 3, 6, 12 hours). (**D**): RNA extracted from a *GAL::nop1* strain following growth on galactose medium ($NOP1^+$) and shift to glucose medium for the time indicated above each lane (24, 48, 72 hours). DNA sequences obtained with the same oligo used for primer extension were run alongside and are also shown. The primer extension stops due to the A0 cleavage are indicated.

its identity is unclear. Pulse-chase labelling of low molecular weight RNA does not reveal any alteration in the ratio of 5.8S long and short forms in either mutant (data not shown).

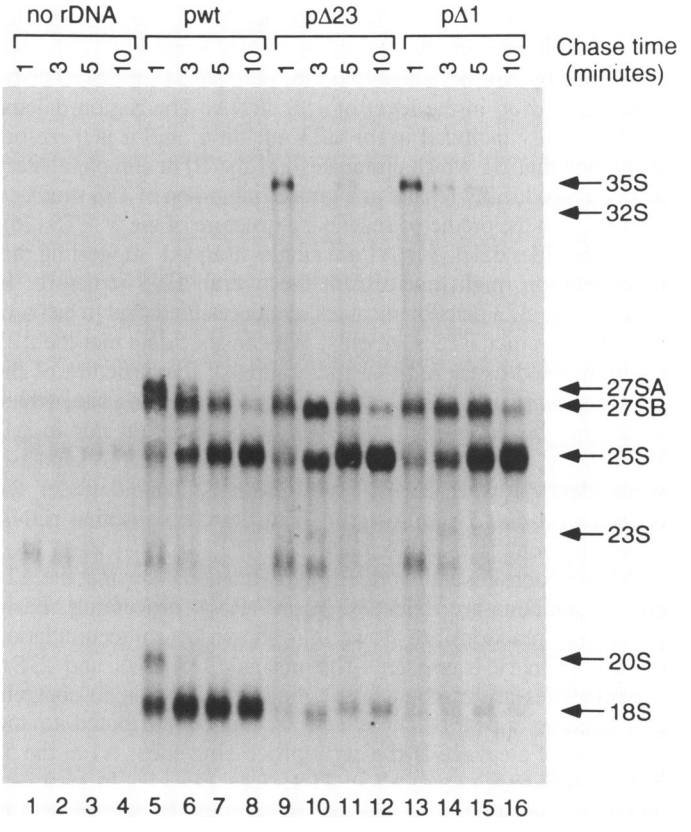

Figure 8. Pulse-chase labeling of pre-rRNA in the Δ23 and Δ1 mutants. Lanes 1–4: RNA extracted from a strain carrying a plasmid lacking the rDNA insert. Lanes 5–8: RNA extracted from a strain carrying pwt. Lanes 9–12: RNA extracted from a strain carrying pΔ23. Lanes 13–16: RNA extracted from a strain carrying pΔ1. All strains carry the pol I ts mutation. Following incubation for 9 hours at 37°C, cells were labelled with [^{3}H-methyl]methionine for 2 min, and then chased with a large excess of unlabelled methionine for the times indicated. RNA was extracted, separated on an agarose-formaldehyde gel and visualized by fluorography. The positions of the processing intermediates and the mature rRNAs are indicated. The identity of the band intermediate in size between 25S and 18S, which is also seen in the no rDNA control samples, is unclear.

DISCUSSION

We have previously shown that the region of the yeast 5′ ETS surrounding a site of *in vivo* cross-linking to U3 snoRNA, is required for the synthesis of mature 18S rRNA (25). Moreover, this region of the yeast ETS has apparent homology to ETS sequences from other eukaryotes (25).

To identify functionally important sites, a set of short deletions spanning the region of potential conservation 3′ to +470 was created *in vitro* (Fig. 2) and inserted in a plasmid which carries the complete pre-rRNA coding sequence fused to a *GAL7* promoter. To assess the effects of the ETS mutations on growth and pre-rRNA processing, these plasmids were introduced into a yeast strain carrying a temperature sensitive lethal mutation in RNA pol I. Following transfer to nonpermissive temperature (37°C), transcription of the chromosomal rDNA is lost. Growth of this strain can be supported by plasmids expressing the wild-type pre-rRNA sequence under the control of the *GAL7* promoter. The deletion of the region of complementarity to U3 snoRNA from the ETS sequence (in the Δ23 and Δ1 mutants) strongly

inhibits growth at 37°C. These data suggested a crucial role for the U3 complementary region in rRNA synthesis. This was confirmed by Northern analysis; the Δ23 and Δ1 mutations cause a dramatic drop in the level of 18S rRNA. The region deleted by Δ1 is fully included in the Δ23 mutation, and it is therefore surprising that Δ1 which eliminates just the 10 nt complementary to U3, reproducibly results in a greater inhibition of 18S synthesis than Δ23. In the predicted secondary structure of the 5′ ETS (26), the nucleotides deleted in Δ1 are single-stranded, suggesting that their deletion might not disrupt the overall ETS structure. In contrast, the Δ23 deletion includes sequences predicted to be base-paired with other ETS segments. We can speculate that the Δ23 deletion could cause a greater alteration of the structure of the 5′ ETS potentially unmasking a cryptical processing site, which would not be accessible in the wild-type situation nor in Δ1. Importantly, the effects of all of the mutations on rRNA synthesis were identical whether expressed from a plasmid under the control of a *GAL7* promoter or from the chromosomal rDNA under the control of RNA pol I.

Primer extension and Northern hybridization show that the Δ23 and Δ1 mutants are defective in pre-rRNA processing. Early processing reactions are slowed, as shown by an accumulation of 35S primary transcript. The normal 32S, 20S and 27SA intermediates are missing in the mutants, whereas an aberrant 23S species appears. These effects can be attributed to the inhibition of cleavage at the early processing sites, A1 at the 5′ end of 18S rRNA and A2 in ITS1 (see Fig. 1). In contrast, processing at other sites, B1(L), B1(S) and C1 (see Fig. 1) is not detectably affected. Cleavage at site A3 in ITS1 is reduced by the D23 mutation, but not by the D1 mutation. Cleavage at sites A1 and A2 is inhibited by the depletion of the snoRNAs snR10, U14, U3, snR30 (9–12) and the associated nucleolar proteins Nop1p, Gar1p, and Sof1p (14–16), leading to the suggestion that they may act in the form of a multi-snoRNP complex implicated in the maturation of 18S rRNA. Cleavage at site A3 requires the RNase MRP RNP complex and is inhibited by mutations in the MRP RNA or Pop1p protein (13), but is not known to require the U3 snoRNP. The reduction in A3 cleavage by the D23 mutation may indicate that factors which play a role in the efficiency of RNase MRP processing also contact the pre-rRNA in the +470 region. Interestingly, A3 cleavage is partially inhibited by cis-acting mutations flanking site A2 (Henry and Tollervey, unpublished), at which the putative multi-snoRNP processing complex presumably also binds.

Depletion of U3 snoRNA inhibits a cleavage in the 5′ ETS at site A0 (11). It was suggested that cleavage at site A0 might involve also other snoRNP components affecting the processing leading to 18S rRNA synthesis (11). We report here that cleavage at A0 is inhibited in strains depleted of Nop1p or Sof1p, but is not affected by the depletion of U14, snR10, snR30 or Gar1p. Nop1p and Sof1p are both components of the U3 snoRNP, whereas Gar1p is a component of the snR10 and snR30 snoRNPs. This indicates that the effect on A0 cleavage is specific for depletion of the U3 snoRNP. The Δ23 and Δ1 deletions also inhibit cleavage at site A0. All the known effects on pre-rRNA processing of U3 depletion in trans are therefore mimicked by deletion of the complementary sequence in the ETS in cis, indicating that we have identified a functional U3 binding site.

In contrast to the effects of the Δ23 and Δ1 mutations, ETS deletions 3′ to the U3 complementary sequence (Δ2, Δ3 and Δ4) have no effect on growth or steady state levels of mature 18S and 25S rRNAs. Moreover, these mutants have normal levels of all pre-rRNA processing intermediates and are not altered in cleavage at any processing site tested. It is worth noting that the Δ2 deletion eliminates 8 nt which are complementary to the 5′ end of snR30; our results indicate that base-pairing of snR30 to this 5′ ETS region is not required for its function.

The interaction between the U3 snoRNP and the pre-rRNA at +470 appears to have an essential role in processing, possibly acting in the assembly of the putative multi-snoRNP complex. The binding of U3 to this site is needed not only for the U3-dependent A0 cleavage, but also for subsequent processing at sites A1 and A2, which lies over 2 kb downstream of the U3 binding site in pre-rRNA. Although all the trans-acting factors are present, the simple deletion of 10 nt in the ETS blocks the processing events. We speculate that this sequence complementarity might direct the initial binding of U3 to the pre-rRNA.

This raises the question of the similarities between U3/ETS interactions in yeast and other eukaryotes. A primer extension stop, which we believe to be due to an ETS cleavage between nt +471 and +472 (underlined in Fig. 2), lies at the 5′ end of the region of U3/ETS complementarity in yeast. Sites of 5′ ETS cleavage have been reported for mouse, human and *Xenopus* cells and these cleavages can be reproduced *in vitro* in mouse and *Xenopus* extracts (18, 19). The regions immediately 3′ to the cleavage sites are required for cleavage of the vertebrate ETS *in vitro* (19, 33) and formation of the terminal balls on the nascent pre-rRNA transcripts in *Xenopus* oocytes (21). A sequence in this region of the mouse 5′ ETS (nt +666 to +672) has 7 nucleotides complementary to a sequence in mouse U3 (nt +64 to +70) (34, 35). Suggestively, the 3′ end of this ETS sequence corresponds to the 3′ end of the region defined as the minimal substrate for *in vitro* processing (33). Complementarity can be found between the human U3 (nt +63 to +69) and human ETS (nt +440 to +446) at a similar, but not identical position (34, 36). In the case of *Xenopus laevis*, a sequence (nt +312 to +319) with potential complementarity to U3 (nt +65 to +72) lies further 3′ to the cleavage site in a short region which is conserved between *X.laevis* and *X.borealis* (17, 37). As in yeast, the vertebrate U3 sequences complementary to the cognate ETS are predicted to be mainly single-stranded. Moreover, in human and *Xenopus* U3 they have been shown to be accessible in the snoRNP particles (17, 36), consistent with their participation in pre-rRNA binding. It is possible that the ability of U3 to base-pair to the ETS 3′ to the cleavage site has been functionally conserved, although the position of the interaction has varied in evolution.

ACKNOWLEDGEMENTS

We would like to thank Elisabeth Petfalski for expert technical assistance, Phil Mitchell, Jaap Venema and Marco E.Bianchi for critical reading of the manuscript. M.B. was partially supported by a grant from the Consiglio Nazionale delle Ricerche (Italy).

REFERENCES

1. Musters,W., Boon,K., van der Sande,C.A.F.M., van Heerikhuizen,H. and Planta,R.J. (1990) *EMBO J.*, 9, 3989–3996.
2. van der Sande,C.A.F.M., Kwa,M., van Nues,R.W., van Heerikhuizen,H., Raué,H.A. and Planta,R.J. (1992) *J. Mol. Biol.*, 223, 899–910.
3. Musters,W., Planta,R.J., van Heerikhuizen,H. and Raué,H.A. (1990) In Hill,W.E., Dahlberg,A.E., Garrett,R.A., Moore,P.B., Schlessinger,D. and

Warner,J.R. (eds.), The Ribosome: Structure, Function and Evolution. Amer. Soc. Microbiol., Washington, DC.
4. van Nues,R.W., Rientjes,J.M.J., van der Sande,C.A.F.M., Zerp,S.F., Sluiter,C., Venema,J., Planta,R.J. and Raué,H.A. (1994) *Nucleic Acids Res.*, 22, 912–919.
5. Henry,Y., Wood,H., Morrissey,J.P., Petfalski,E., Kearsey,S. and Tollervey,D. (1994) *EMBO J.*, 13, 2452–2463.
6. Fournier,M.J. and Maxwell,E.S. (1993) *Trends Biochem. Sci.*, 18, 131–135.
7. Terns,M.P. and Dahlberg,J.E. (1994) *Science*, 264, 959–961.
8. Sollner-Webb,B. (1993) *Cell*, 75, 403–405.
9. Tollervey,D. (1987) *EMBO J.*, 6, 4169–4175.
10. Li,H.V., Zagorski,J. and Fournier,M.J. (1990) *Mol. Cell. Biol.*, 10, 1145–1152.
11. Hughes,J.M.X. and Ares,M.J. (1991) *EMBO J.*, 10, 4231–4239.
12. Morrissey,J.P. and Tollervey,D. (1993) *Mol. Cell. Biol.*, 13, 2469–2477.
13. Lygerou,Z., Mitchell,P., Petfalski,E., Séraphin,B. and Tollervey,D. (1994) *Genes & Dev.*, 8, 1423–1433.
14. Tollervey,D., Lehtonen,H., Carmo-Fonseca,M. and Hurt,E.C. (1991) *EMBO J.*, 10, 573–583.
15. Girard,J.-P., Lehtonen,H., Caizergues-Ferrer,M., Amalric,F., Tollervey,D. and Lapeyre,B. (1992) *EMBO J.*, 11, 673–682.
16. Jansen,R.P., Tollervey,D. and Hurt,E.C. (1993) *EMBO J.*, 12, 2549–2558.
17. Savino,R. and Gerbi,S.A. (1990) *EMBO J.*, 9, 2299–2308.
18. Kass,S., Tyc,K., Steitz,J.A. and Sollner-Webb,B. (1990) *Cell*, 60, 897–908.
19. Mougey,E.B., Pape,L.K. and Sollner-Webb,B. (1993) *Mol. Cell. Biol.*, 13, 5990–5998.
20. Kass,S. and Sollner-Webb,B. (1990) *Mol. Cell. Biol.*, 10, 4920–4931.
21. Mougey,E.B., O'Reilly,M., Osheim,Y., Miller,O.L.J., Beyer,A. and Sollner-Webb,B. (1993) *Genes & Dev.*, 7, 1609–1619.
22. Saffer,L.D. and Miller,O.L.J. (1986) *Mol. Cell. Biol.*, 6, 1148–1157.
23. Stroke,I.L. and Weiner,A.M. (1989) *J. Mol. Biol.*, 210, 497–512.
24. Maser,R.L. and Calvet,J.P. (1989) *Proc. Natl. Acad. Sci. USA*, 86, 6523–6527.
25. Beltrame,M. and Tollervey,D. (1992) *EMBO J.*, 11, 1531–1542.
26. Yeh,L.-C.C. and Lee,J.C. (1992) *J. Mol. Biol.*, 228, 827–839.
27. Ségault,V., Mougin,A., Grégoire,A., Banroques,J. and Branlant,C. (1992) *Nucleic Acids Res.*, 20, 3443–3451.
28. Nogi,Y., Yano,R., Dodd,J., Carles,C. and Nomura,M. (1993) *Mol. Cell. Biol.*, 13, 114–122.
29. Landt,O., Grunert,H.-P. and Hahn,U. (1990) *Gene*, 96, 125–128.
30. Nogi,Y., Ryoji,Y. and Nomura,M. (1991) *Proc. Natl. Acad. Sci. USA*, 88, 3962–3966.
31. Ito,H., Fukuda,Y., Murata,K. and Kimura,A. (1983) *J. Bacteriol.*, 153, 163–168.
32. Musters,W., Venema,J., van der Linden,G., van Heerikhuizen,H., Klootwijk,J. and Planta,R.J. (1989) *Mol. Cell. Biol.*, 9, 551–559.
933. Craig,N., Kass,S. and Sollner-Webb,B. (1991) *Mol. Cell. Biol.*, 11, 458–467.
34. Kass,S., Craig,N. and Sollner-Webb,B. (1987) *Mol. Cell. Biol.*, 7, 2891–2898.
35. Mazan,S. and Bachellerie,J.-P. (1988) *J. Biol. Chem.*, 263, 19461–19467.
36. Parker,K.A. and Steitz,J.A. (1987) *Mol. Cell. Biol.*, 7, 2899–2913.
37. Furlong,J.C., Forbes,J., Robertson,M. and Maden,B.E.H. (1983) *Nucleic Acids Res.*, 11, 8183–8196.